JACS
JOURNAL OF THE AMERICAN CHEMICAL SOCIETY
Article
pubs.acs.org/JACS

Intermolecular N−H Oxidative Addition of Ammonia, Alkylamines, and Arylamines to a Planar σ^3-Phosphorus Compound via an Entropy-Controlled Electrophilic Mechanism

Sean M. McCarthy,[†] Yi-Chun Lin,[†] Deepa Devarajan,[‡] Ji Woong Chang,[§] Hemant P. Yennawar,[†] Robert M. Rioux,[§] Daniel H. Ess,*[,‡] and Alexander T. Radosevich*[,†]

[†]Department of Chemistry, The Pennsylvania State University, University Park, Pennsylvania 16802, United States
[§]Department of Chemical Engineering, The Pennsylvania State University, University Park, Pennsylvania 16802, United States
[‡]Department of Chemistry and Biochemistry, Brigham Young University, Provo, Utah 84602, United States

Supporting Information

ABSTRACT: Ammonia, alkyl amines, and aryl amines are found to undergo rapid intermolecular N−H oxidative addition to a planar mononuclear σ^3-phosphorus compound (**1**). The pentacoordinate phosphorane products (**1**·[H][NHR]) are structurally robust, permitting full characterization by multinuclear NMR spectroscopy and single-crystal X-ray diffraction. Isothermal titration calorimetry was employed to quantify the enthalpy of the N−H oxidative addition of *n*-propylamine to **1** (^{n}PrNH$_2$ + **1** → **1**·[H][NH^{n}Pr], ΔH_{rxn}^{298} = −10.6 kcal/mol). The kinetics of *n*-propylamine N−H oxidative addition were monitored by in situ UV absorption spectroscopy and determination of the rate law showed an unusually large molecularity ($\nu = k[\mathbf{1}][^n\mathrm{PrNH_2}]^3$). Kinetic experiments conducted over the temperature range of 10−70 °C revealed that the reaction rate decreased with increasing temperature. Activation parameters extracted from an Eyring analysis ($\Delta H^{\ddagger}$ = −0.8 ± 0.4 kcal/mol, $\Delta S^{\ddagger}$ = −72 ± 2 cal/(mol·K)) indicate that the cleavage of strong N−H bonds by **1** is entropy controlled due to a highly ordered, high molecularity transition state. Density functional calculations indicate that a concerted oxidative addition via a classical three-center transition structure is energetically inaccessible. Rather, a stepwise heterolytic pathway is preferred, proceeding by initial amine-assisted N−H heterolysis upon complexation to the electrophilic phosphorus center followed by rate-controlling N → P proton transfer.

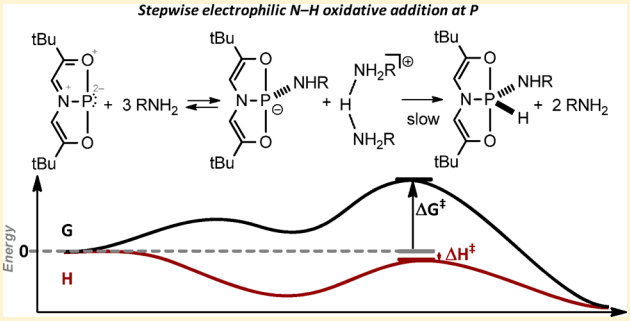

1. INTRODUCTION

The homogeneous activation of N−H bonds is of significant interest in connection with the direct catalytic functionalization of ammonia and amine derivatives for a broad range of applications.[1] The activation of N−H bonds by oxidative addition to transition metals has been a prime focus of investigation. For instance, Goldman and Hartwig[2] have described the addition of ammonia to an iridium(I) pincer complex (Figure 1A), and related examples of N−H cleavage reactions have been characterized for a range of early,[3] late,[4] and polynuclear transition complexes.[5]

In line with a growing interest in catalysis with abundant nonprecious elements,[6] recent advances in fundamental bond activation chemistry have shown the cleavage of strong covalent bonds is possible by persistent main group compounds under mild homogeneous conditions.[7−9] With respect to N−H bond cleavage, Bertrand and Schoeller have demonstrated that nucleophilic singlet carbenes are capable of ammonia N−H cleavage under ambient conditions (Figure 1B).[10] Bielawski and Siemeling have documented similar reactivity with electronically diverse carbenes,[11] and related N−H oxidative addition chemistry has been observed with the heavier persistent divalent group 14 compounds (i.e., silylenes, germylenes, stannylenes)[12] by Power[13] and Roesky.[14] Alternative heterolytic N−H activation strategies including ligand−

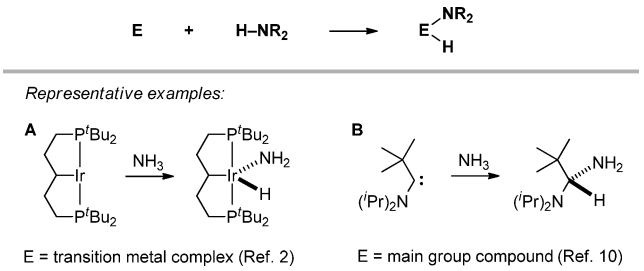

Figure 1. Intermolecular N−H oxidative addition by (A) a transition metal complex and (B) a nonmetal ccompound.

Received: December 7, 2013
Published: March 5, 2014

   dx.doi.org/10.1021/ja412469e | J. Am. Chem. Soc. 2014, 136, 4640−4650

metalloid cooperativity[15] and Lewis acid/base pairing[16] have also been demonstrated.

Nonmetal group 15 compounds have the potential to provide unique geometric structures and electronics for bond cleavage reactions. The tricoordinate phosphorus compound **1**, initially described by Arduengo (Figure 2),[17] displays an

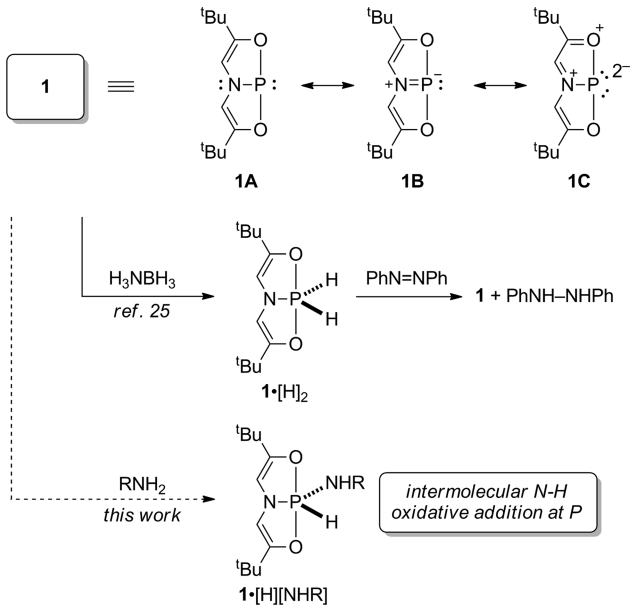

Figure 2. Resonance structures, ammonia-borane dehydrogenation, and amine N–H bond oxidative addition by compound **1**.

unusual planar T-shaped geometry at phosphorus with the tridentate O,N,O-binding motif occupying three adjacent coplanar sites. The electronic structure of this compound has been extensively investigated by Arduengo and Dixon.[18] As in related delocalized heterocyclic systems,[19] the pincer-like T-shaped geometry[20,21] is stabilized by extensive mesomerism in the π-plane of the molecule (e.g., resonance structures **1A–C**); several lines of spectroscopic and theoretical evidence suggest **1C** is a significant contributor to the overall electronic structure. The reactivity of this compound with respect to certain small molecule substrates (including Bronsted acids, alcohols, halogens, quinones and electron-deficient alkynes)[22] and transition metal complexation[23] has been investigated by Arduengo. More recently, Driess has described the nucleophilic addition of **1** to methyl triflate.[24]

Recently, one of our groups has demonstrated that **1** can serve as a platform for catalytic transfer hydrogenation via the intermediacy of a pentacoordinate dihydridophosphorane (**1**·$[H]_2$) formed from the dehydrogenation of ammonia-borane (Figure 2).[25] Among the possible mechanistic courses, we considered that the formation of **1**·$[H]_2$ might proceed via an initial N–H oxidative addition to phosphorus. Intramolecular N–H oxidative addition by P(III) $\rightleftarrows$ P(V) ring–chain tautomerism is well-known, and structural factors controlling the position of this reversible cyclization equilibrium have been discussed.[26] Intermolecular N–H oxidative addition to phosphorus, by contrast, is less well-characterized due to instability of the P(V) adducts toward subsequent reductive elimination. The only well-characterized examples of intermolecular oxidative addition of N–H bonds to tricoordinate phosphorus resulting in isolable phosphorane adducts involve the addition of amines to substituted difluorophosphines RPF_2 to yield difluorophosphoranes.[27] Additional in situ spectral evidence exists for intermolecular N–H oxidative addition giving hydrido amido phosphoranes as persistent intermediates in (1) the substitution reaction of trivalent phosphorus electrophiles with amines to yield P(III) amides,[28] and (2) the reaction of $P(NMe_2)_3$ with diethanolamines en route to fused bicyclic phosphoramidites.[29] With respect to attempted N–H oxidative addition to **1** itself, Arduengo has noted that dimethylamine fails to give an adduct with **1**, although the same report does document the O–H oxidative addition product **1**·[H][OMe] as an observable metastable intermediate in the methanolysis of **1**.[22a]

In this manuscript, we demonstrate intermolecular N–H bond cleavage of ammonia, alkylamines, and arylamines by oxidative addition to tricoordinate phosphorus compound **1** proceeding under mild homogeneous conditions and leading to structurally robust adducts that permit full spectroscopic and crystallographic characterization. The fidelity and velocity of these reactions enable quantification of both the reaction enthalpy and kinetics. Together with these experimental results, theoretical calculations indicate that the N–H oxidative addition reaction proceeds in a heterolytic stepwise fashion initiated by electrophilic reactivity of **1**. In view of the typical Lewis basicity of tricoordinate phosphorus, these results illustrate the extent to which unusual electronic structure arising from geometric distortion can lead to high reactivity in the main group.[30]

2. RESULTS

2.1. Synthesis and Characterization. *2.1.1. Addition of Ammonia.* To initiate the investigation of N–H oxidative addition, ammonia was condensed onto a solid sample of **1** at −78 °C (Figure 3). After 30 min, the NH_3 was removed under

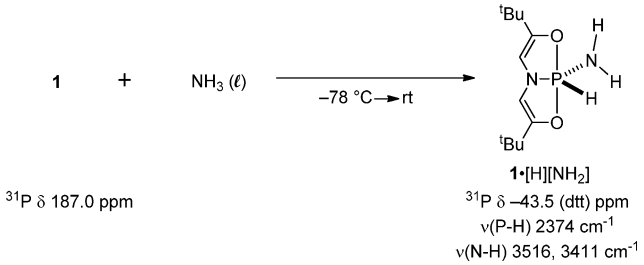

Figure 3. Ammonia oxidative addition to **1**.

an N_2 sweep yielding a crude solid, which was dissolved in C_6D_6. NMR analysis indicated full consumption of **1** (^{31}P δ 187.0 ppm) and clean conversion to a single new phosphorus containing product with a ^{31}P NMR resonance centered at δ −43.5 ppm, consistent with formation of a pentacoordinate phosphorus species.[31]

The signal multiplicity (Figure 4, bottom) further suggests an addition reaction with ammonia, and the largest value of J = 812 Hz is indicative of direct $^1J_{PH}$ coupling (longer range $^3J_{PH}$ coupling to the vinylic ligand C–H protons (31.1 Hz) and $^2J_{PH}$ coupling to the N–H protons (10.2 Hz) is also evident). The complementary P–H coupling observed in the ^1H NMR spectrum corroborates this assignment (Figure 4, top); specifically, a phosphorus-coupled doublet for the P–H is found at δ 8.79 ppm ($^1J_{PH}$ = 812 Hz). Additionally, a feature at 2374 cm^{-1} in the infrared spectrum may be assigned to the stretching mode of a P–H unit, and two bands observed in the

dx.doi.org/10.1021/ja412469e | J. Am. Chem. Soc. 2014, 136, 4640–4650

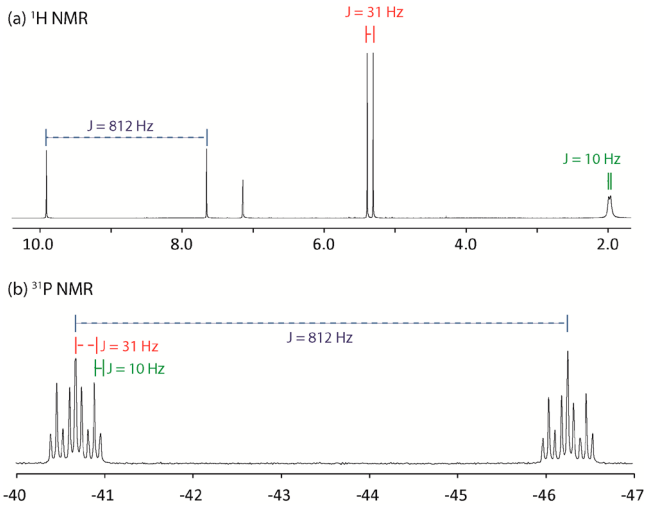

Figure 4. (a) Abridged annotated ^{1}H NMR spectrum for **1**·[H][NH_2] in C_6D_6. An additional ^{1}H signal for $-C(CH_3)_3$ is found at δ 1.06 ppm. (b) Annotated ^{31}P NMR spectrum for **1**·[H][NH_2] in C_6D_6. Units are ppm relative to Me_4Si (^{1}H) and H_3PO_4 (^{31}P). See Supporting Information for full spectra.

infrared spectrum at 3516 and 3411 cm^{-1} are consistent with the symmetric and antisymmetric stretching bands of a terminal $-NH_2$ group.

Taken together, these spectroscopic details are consistent with the formation of an authentic N−H bond cleavage product **1**·[H][NH_2] resulting from the reaction of ammonia and **1**.[32] According to Martin's empirical correlation between $^1J_{PH}$ and ligand electronegativity,[33] the observed coupling constant is best accommodated by a trigonal bipyramidal structure for **1**·[H][NH_2] having an equatorial hydride and amide as depicted in Figure 3.

2.1.2. Addition of Alkyl Amines. Exposure of **1** to primary alkyl amines similarly leads to N−H bond cleavage (Figure 5). For instance, the addition of 1 equiv of *n*-propylamine to a benzene-d_6 solution of **1** in a sealable NMR tube at ambient temperature results in quantitative conversion of **1** to hydrido propylamido phosphorane **1**·[H][NH^{n}Pr] (δ −46.4 ppm, J = 815 Hz). This reaction is rapid, proceeding to completion within minutes of mixing. No intermediates are evident in either the ^{1}H or ^{31}P NMR spectra. Analogous reactivity was observed with other primary aliphatic amines, giving **1**·[H][NH^{i}Pr] (δ −47.1 ppm, J = 819 Hz) and **1**·[H][NHBn] (δ −46.0 ppm, J = 824 Hz) by the addition of isopropylamine and benzylamine, respectively.

2.1.3. Addition of Aryl Amines. Reaction of **1** with *p*-anisidine was also found to yield hydrido anilido phosphorane **1**·[H][NHPMP] (δ −48.7 ppm, J = 831 Hz) by oxidative addition (Figure 5); however, the qualitative rate of reaction in this case is somewhat decreased relative to the primary alkyl amines. This effect is especially pronounced with more sterically encumbered anilines. Specifically, the reaction of 2,6-disubstituted anilines with **1** in benzene solution proceeds only sluggishly at ambient temperature, but heating the mixture in a sealed NMR tube at 55 °C results in complete conversion over 2 h. Under these conditions, both 2,4,6-trimethylaniline and 2,6-diisopropylaniline were observed to give the corresponding hydrido anilido phosphoranes **1**·[H][NHMes] (δ −48.9 ppm, J = 840 Hz) and **1**·[H][NHDipp] (δ −51.4 ppm, J = 841 Hz).

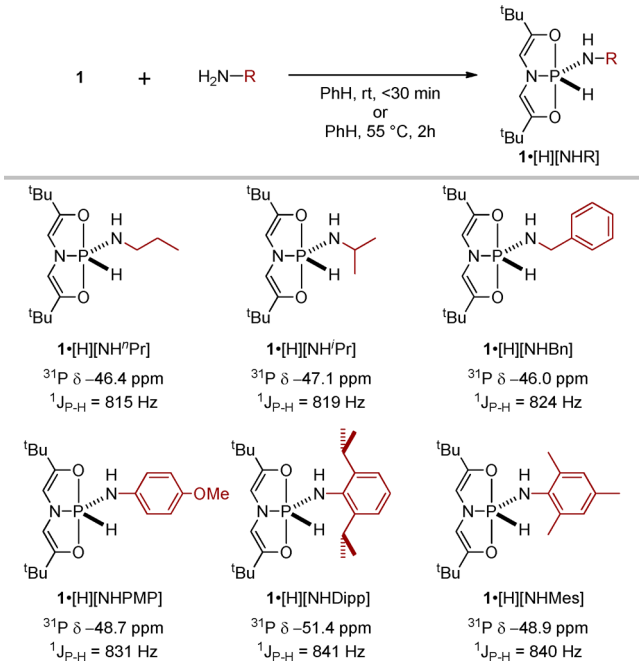

Figure 5. Examples of intermolecular N−H oxidative addition of alkyl and aryl amines to **1**. Reactions with 2,6-disubstituted arylamines were conducted at 55 °C.

2.1.4. Structure and Bonding of N−H Addition Product. A diffraction quality single crystal of **1**·[H][NHMes] was prepared from a concentrated pentane solution following filtration over neutral alumina. As depicted in the thermal ellipsoid plot in Figure 6, this N−H cleavage adduct adopts an

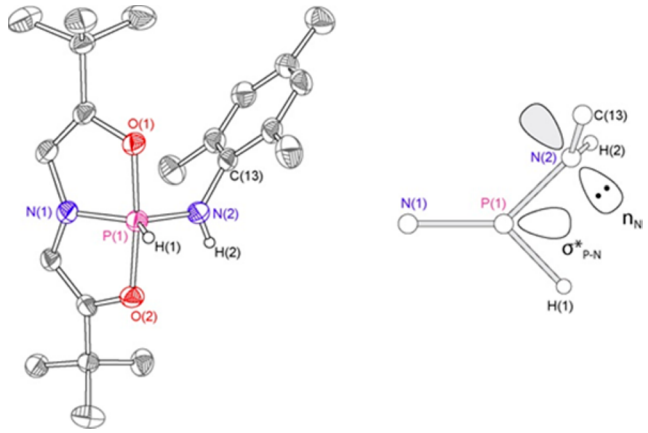

Figure 6. (Left) Molecular structure of **1**·[H][NHMes]. All hydrogen atoms on carbon are omitted for clarity. Thermal ellipsoids are shown at the 50% probability level. (Right) Top view of equatorial plane with schematic orbital representation of $n_N \rightarrow \sigma^*_{P-N}$ interaction .

essentially trigonal bipyramidal monomeric structure about phosphorus in which the O,N,O-chelating motif retains an approximately planar pincer-like arrangement about phosphorus, with oxygen atoms spanning apical positions at an O−P−O angle of 174.0(1)°. When compared to the parent compound **1**, the supporting ligand in **1**·[H][NHMes] exhibits a significant contraction in both P−O and P−N1 bond distances (the relevant structural metrics are tabulated in Table 1), in line with the increase in valency. The addend nitrogen (N2) and hydrogen (H1) atoms occupy equatorial positions of the

dx.doi.org/10.1021/ja412469e | J. Am. Chem. Soc. 2014, 136, 4640−4650

Table 1. Comparison of Selected Crystallographic Bond Lengths (Å) and Angles (deg) for 1 and 1·[H][NHMes]

metric	1[a]	1·[H][NHMes][b]
P1−O1	1.792(2)	1.703(1)
P1−O2	1.835(2)	1.726(1)
P1−N1	1.703(2)	1.674(1)
P1−N2	-	1.645(1)
P1−H1	-	1.314(15)
O1−P1−O2	167.7(1)	174.0(1)
N1−P1−N2	-	123.3(1)
N1−P1−H1	-	123.7(7)

[a]Data from ref 17. [b]See Supporting Information for full crystallographic details.

trigonal bipyramid (P1−N2 = 1.645(1) Å, P1−H1 = 1.315(15) Å) along with N1 of the bicyclic supporting structure. The hydrogen atoms on P and N2 could be detected in the experimental electron density map and were refined isotropically. In accord with Bent's rule,[34] the substituents around the phosphorane-bound anilide nitrogen atom N2 are found to be planarized. The orientation of the coordination plane around N2 is disposed orthogonally with respect to the equatorial plane at phosphorus, indicative of a stabilizing interaction with phosphorus (likely via $n_{N2} \rightarrow \sigma^*_{(P-N1)}$[35] as in Figure 5) and is consistent with the well-known preference for π-donor substituents to occupy the equatorial plane of pentacoordinate phosphorus.[36] An NBO analysis[37] of 1·[H][NHMes] substantiates this orbital interaction (see Supporting Information for details).

2.2. Thermodynamic and Mechanistic Investigations. *2.2.1. Enthalpy of N−H Oxidative Addition.* In an effort to ascertain the driving force for N−H oxidative addition to **1**, we have undertaken thermodynamic investigations using isothermal titration calorimetry (ITC). ITC experiments were carried out by titration of a solution of **1** (1 mM in PhH, 1 mL total volume) with 6 μL aliquots of an *n*-propylamine solution (12.5 mM in PhH) at 25 °C under an inert atmosphere. Figure 7 shows an isotherm for the addition of *n*-propylamine to **1** (top) and the integrated heats measured by ITC (bottom). Utilizing an independent binding site model (red line in Figure 7), we confirm a 1:1 stoichiometry for the binding of *n*-propylamine to **1**. An enthalpy of reaction of −10.6 ± 0.1 kcal/mol and an equilibrium constant of (3.03 ± 0.17) × 10^4 M^{-1} were extracted from the independent binding sites model.

Experimental data regarding bond energies in hydridophosphoranes are limited; therefore, the P−H and P−N strengths in 1·[H][NH^{n}Pr] were estimated with calculations. In accordance with the ITC values, M06-2X/6-311++G(2d,2p) calculations estimate ΔH_{298} = −7.4 kcal/mol. The homolytic P−H and P−N bond dissociation energies (ΔH_{298}) were computed using a model of 1·[H][NH^{n}Pr] (Figure 8). The computed phosphoranyl radicals arising from P−H and P−N bond scission exhibit seesaw (monovacant trigonal bipyramidal) structures with minimal structural reorganization of the remaining substituents. The calculated P−H bond dissociation energy is D_{P-H} = 70.6 kcal/mol, which for comparison is somewhat less than the experimental value for trivalent PH_3 (D_{P-H} = 83.9 ± 0.5 kcal/mol)[38] but is consistent with Bentrude's observation of radical P−H abstraction in a hydridophosphorane by thiyl radicals.[39] The calculated P−N bond dissociation energy (D_{P-N} = 68.3 kcal/mol) is in line with the experimental values obtained for both trivalent (D_{P-N} = 66.8 ± 0.8 kcal/mol in $P(NEt_2)_3$)[40] and

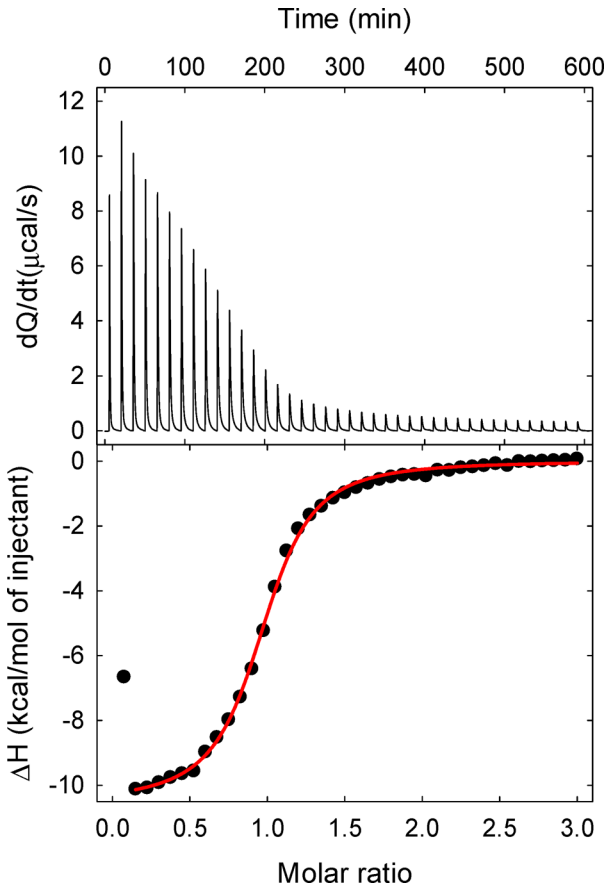

Figure 7. Thermochemistry of N−H oxidative addition of *n*-propylamine to **1**. (Top) ITC thermogram at 25 °C in benzene. (Bottom) Plot of integrated heat evolved with fitted model.

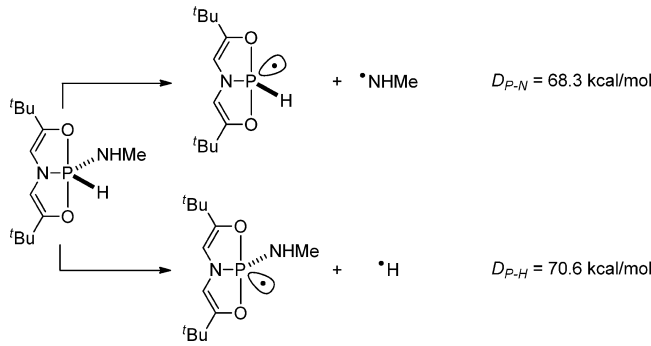

Figure 8. M06-2X/6-311++G(2d,2p) P−H and P−N bond enthalpies.

pentavalent (D_{P-N} = 74.3 kcal/mol in $(Cl_3PNMe)_2$)[41] phosphorus compounds.

2.2.2. Attempted Reductive Elimination and Amine Exchange Experiments. Attempts to promote the reductive elimination of amine from several adducts 1·[H][NHR] by heating solid samples in vacuo at elevated temperature have been unsuccessful to date. For instance, ammonia adduct 1·[H][NH_2] sublimes without decomposition at 40 °C and 1 mmHg. Similarly, heating of heavier amine adducts such as 1·[H][NHMes] to higher temperatures under vacuum does not drive reductive elimination, but results instead only in nonspecific decomposition.

By contrast, heating adducts 1·[H][NHR] with an excess of an exogenous amine H_2NR' in benzene solution leads to amine

dx.doi.org/10.1021/ja412469e | J. Am. Chem. Soc. 2014, 136, 4640−4650

ligand exchange. Specifically, exposure of a benzene solution of **1**·[H][NH^{n}Pr] to 5 equiv. of benzylamine (H_2NBn) for 24 h at 80 °C in a sealed NMR tube results in formation of **1**·[H][NHBn] (Figure 9). Likewise, when a benzene solution of **1**·[H][NHBn] is heated with 5 equiv *n*-propylamine (H_2N^nPr) at 80 °C in a sealed NMR tube, **1**·[H][NH^{n}Pr] is observed.

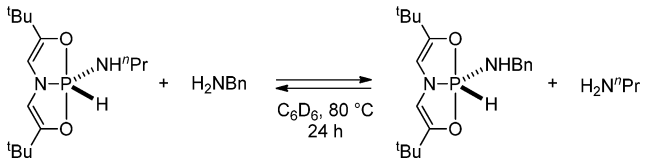

Figure 9. Amine exchange in benzene solution.

2.2.3. Isotopic Tracer Study. We have employed isotopic labeling experiments to track the course of the N–H bond. Specifically, the presence of the electron-rich O,N,O-supporting structure in **1** suggested the potential for a phosphorus-ligand cooperative mechanism for this oxidative addition. However, exposure of **1** to deuterated benzylamine (D_2NBn) affords deuterated **1**·[D][NDBn] (δ −47.0 ppm, $^1J_{PD}$ = 126 Hz) and related isotopologues with incorporation of isotopic label exclusively at the phosphorus and nitrogen centers (Figure 10).

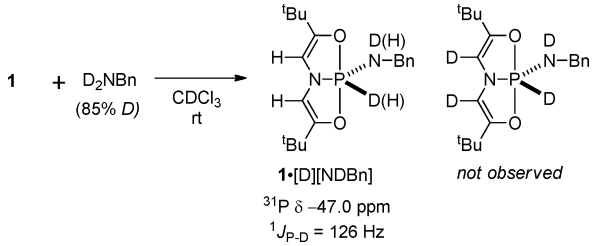

Figure 10. Oxidative addition of N-deuterated benzylamine proceeds without incorporation of the isotopic label in the O,N,O-chelating framework.

The lack of deuteration at the vinylic C–H positions evident in the ^{2}H NMR spectrum makes an active functional role for the O,N,O-supporting structure unlikely; instead, an oxidative addition with reactivity localized at the phosphorus center appears to be operative.

2.2.4. Kinetic Study of N–H Oxidative Addition. An interrogation of the kinetics of the N–H oxidative addition process by in situ UV absorption spectroscopy has permitted an experimental determination of the rate law and related activation parameters. Tricoordinate **1** exhibits electronic absorption features (Figure 11A) at 313 nm (ε = 7.9 × 10^3 M^{-1}·cm^{-1}), 220 nm (ε = 10.5 × 10^3 M^{-1}·cm^{-1}), and 207 nm (ε = 10.5 × 10^3 M^{-1}·cm^{-1}). On the computational model of **1** shown in Figure 11, TDDFT calculations indicate that the low energy band is dominated by $\pi \rightarrow \pi^*$ and $n_P \rightarrow \pi^*$ electronic transitions (the CAMB3LYP/6-311++G** method was used for TDDFT calculations due to significant charge-transfer regions for excitation; see Supporting Information for full details). Oxidative addition of *n*-propylamine to **1** gives the pentacoordinate hydrido amide **1**·[H][NH^{n}Pr], in which the lowest energy band is shifted hypsochromically to 239 nm (ε = 6.7 × 10^3 M^{-1}·cm^{-1}). The progress of the oxidative addition process can therefore be conveniently monitored at λ = 313 nm.

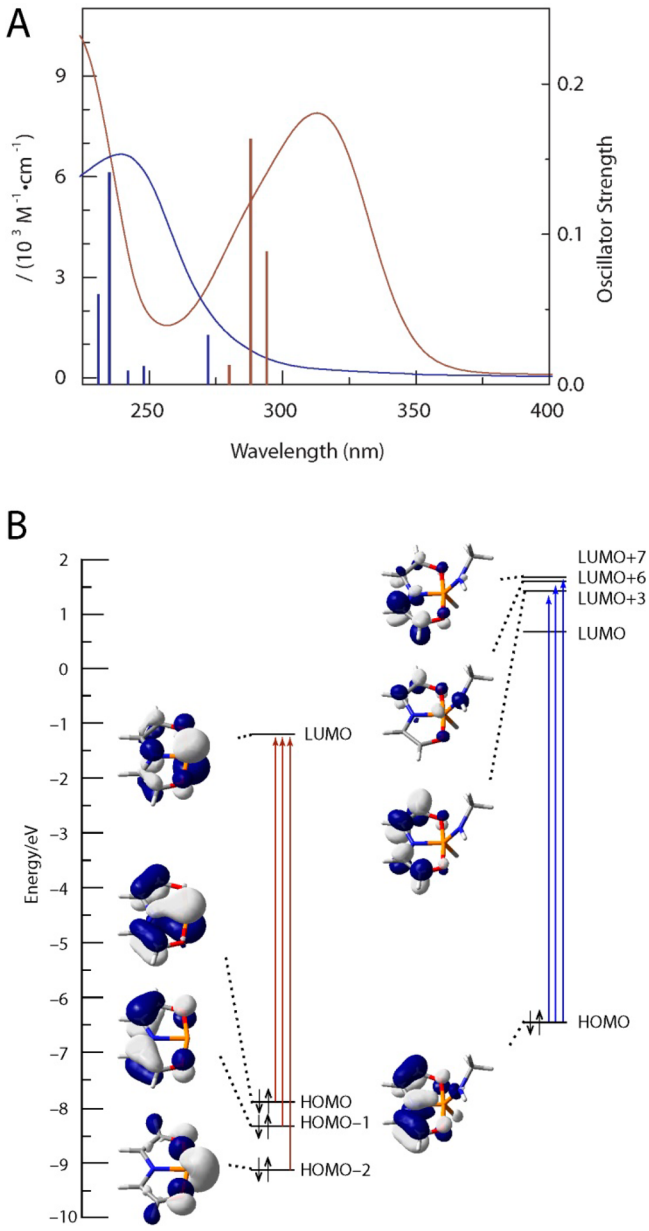

Figure 11. (A) Experimental electronic absorption spectra for **1** (red line) and **1**·[H][NH^{n}Pr] (blue line) superimposed with corresponding TDDFT (CAMB3LYP/6-311++G**) excited state transitions and oscillator strengths. (B) Molecular orbital isosurfaces and energies for models of **1** and **1**·[H][NH^{n}Pr]. See Supporting Information for details.

Kinetic experiments were conducted on solutions of **1** in dry benzene (0.27 mM) in sealable quartz cuvettes. In the presence of at least a 10-fold excess of *n*-propylamine, the N–H oxidative addition reaction proceeds cleanly to **1**·[H][NH^{n}Pr] within minutes and without intervention of observable intermediates or side products (Figure 12A). Under these conditions, kinetic plots follow a pseudo first-order decay with respect to consumption of **1** (Figure 12B). Variation of the concentration of *n*-propylamine (4.3–689 mM, 14–2222 equiv) shows that the pseudo-first order rate constants depend linearly on [H_2N^nPr]^3 (Figure 12C). Thus, the experimentally determined rate law is given by eq 1:

dx.doi.org/10.1021/ja412469e | J. Am. Chem. Soc. 2014, 136, 4640–4650

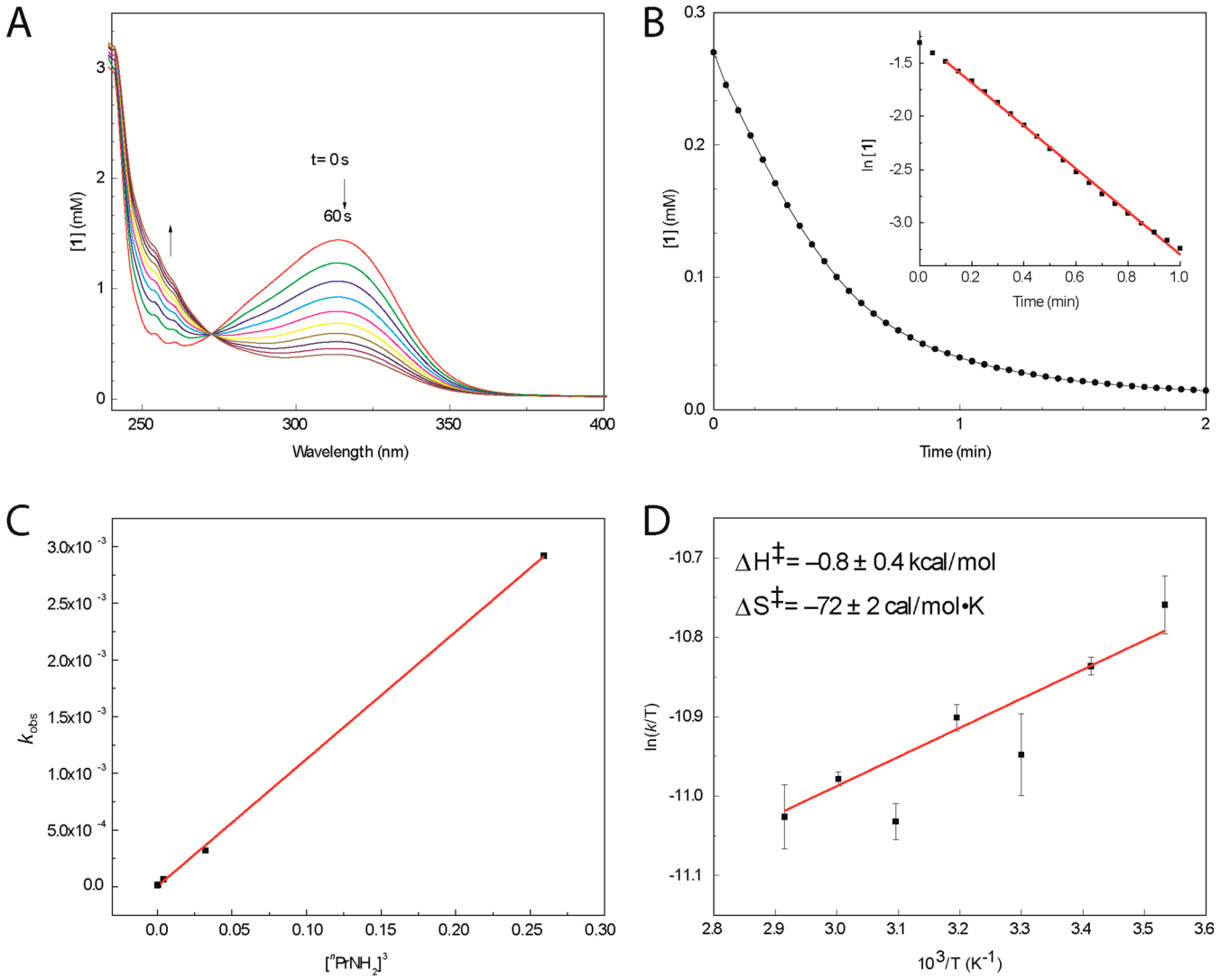

Figure 12. Mechanistic data for the oxidative addition of ^{n}PrNH$_2$ to **1** in PhH. (A) Time stacked absorption spectra indicating consumption of **1** and formation of **1**·[H][NH^{n}Pr] with time. (B) Plot of [**1**] vs time monitored at λ_{max}(**1**) = 314 nm. (Inset) Plot of ln [**1**] vs time with linear least-squares fit. (C) Plot of k_{obs} vs [^{n}PrNH$_2$]^3 with linear least-squares fit. (D) Eyring plot for kinetic data collected over the temperature range 10−70 °C.

$$\frac{-\mathrm{d}[\mathbf{1}]}{\mathrm{d}t} = k'[\mathbf{1}][\mathrm{H_2N}^n\mathrm{Pr}]^3 = k_{obs}[\mathbf{1}] \quad (1)$$

An Eyring plot was constructed for kinetic data collected in at least triplicate at 10 °C temperature intervals between 10 and 70 °C (Figure 12D). Unexpectedly, the observed reaction rate was found to decrease with increasing temperature. The activation parameters extracted from least-squares treatment of the relationship of ln k'/T vs $1/T$ (Figure 12) yield values of $\Delta H^{\ddagger}$ = −0.8 ± 0.4 kcal/mol and $\Delta S^{\ddagger}$ = −72 ± 2 cal/(mol·K).

2.3. DFT Energy Landscape. It is evident from the kinetics investigations (i.e., large molecularity of the experimental rate law, large negative entropy of activation) that the oxidative addition reaction under study here does not proceed by a concerted mechanism via a three-centered transition state.[42] Indeed, a calculated transition structure (M062X, 6-311++G(2d,2p)) corresponding to the concerted process (**TS-conc**, Figure 13) resides at high energy ($\Delta H^{\ddagger}$ = 50.1 kcal/mol). The relatively high barrier to concerted N−H cleavage can be rationalized within the valence bond configurational mixing framework,[43] where the large singlet−triplet gap for **1** (ΔE_{ST} = 62.6 kcal/mol) imposes a large electronic barrier to direct oxidative addition.

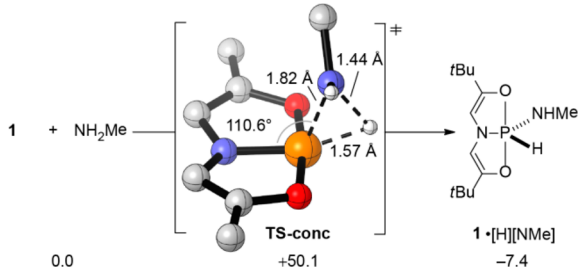

Figure 13. Concerted N−H oxidative addition to **1** with computed metrics and enthalpies in kcal/mol. Hydrogens and *t*-butyl methyl groups were omitted for clarity in **TS-conc**.

We therefore examined two polar stepwise mechanisms differing in the sequence of bond forming events (Figure 14): (A) a nucleophilic mechanism involving initial P−H formation by proton transfer to **1** to yield a phosphonium intermediate, followed by subsequent P−N bond formation, and (B) an electrophilic mechanism involving initial P−N formation by

dx.doi.org/10.1021/ja412469e | J. Am. Chem. Soc. 2014, 136, 4640−4650

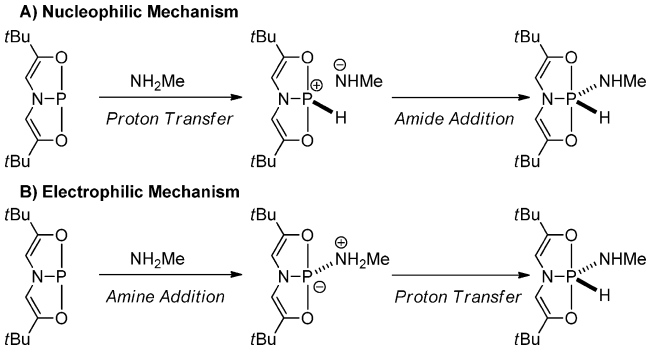

Figure 14. Outline of polar stepwise pathways.

amine addition to **1**, followed by subsequent P−H bond formation.

Calculations indicate that deprotonation of the weakly acidic methylamine substrate by compound **1**, as in pathway A, is energetically prohibitive. Electronically, this fact is suggested in the relatively low energies of the filled frontier orbitals (−7.5, −7.9, and −8.7 eV; for HOMO, HOMO−1 and HOMO−2, respectively) and a large computed ionization potential (IP = 6.4 eV). The reaction enthalpy for the proton transfer to **1** from a single methylamine molecule is ΔH = 87.7 kcal/mol. A marginal decrease in enthalpy is found by the inclusion of additional explicit methylamine molecules. The unfavorable thermodynamics of all these proton transfer events effectively rule out the nucleophilic pathway A shown in Figure 14.[44]

The presence of a low-lying LUMO (−1.0 eV) and the relatively favorable electron affinity (EA = −2.2 eV) indicate that **1** may, by contrast, exhibit electrophilic character. Indeed, examination of a stepwise electrophilic pathway (Figure 15) reveals a significantly lower energy pathway compared to either the concerted pathway or nucleophilic pathway. While attempts to identify a stable P−N adduct between **1** and a single methylamine molecule failed, inclusion of two additional explicit methylamine molecules allowed location of an adduct (**INT1**) with a P−N distance of 1.97 Å (Figure 15). **INT1** is exothermic by −3.8 kcal/mol relative to compound **1** and a hydrogen-bonding cluster of three methylamine molecules on the enthalpy surface but is endergonic by 10.1 kcal/mol on the free energy surface, suggesting that this complex would not be long-lived. Subsequent deprotonation of the phosphorus-bound amine then gives **INT2**, an amidophosphoranide anion[45] and amine-stabilized ammonium cation pair, via **TS1**. The potential energy surface along reaction coordinate **INT1** → **TS1** → **INT2** is found to be quite flat, with $\Delta H^{\ddagger}$ = −2.2 kcal/mol and $\Delta G^{\ddagger}$ = 13.0 kcal/mol for **TS1**. The partial P−N and N−H bond lengths (1.83 and 1.36 Å, respectively) in **TS1** are very similar to those found in **TS-conc**. This observation suggests that the main stabilizing effect in **TS1** is the basicity of the two explicit methylamine molecules involved in hydrogen bonding.

After the P−N bond is formed in **INT2**, the methylammonium reorients and then protonates the phosphoranide center via **TS2** (Figure 16) with a small calculated activation enthalpy

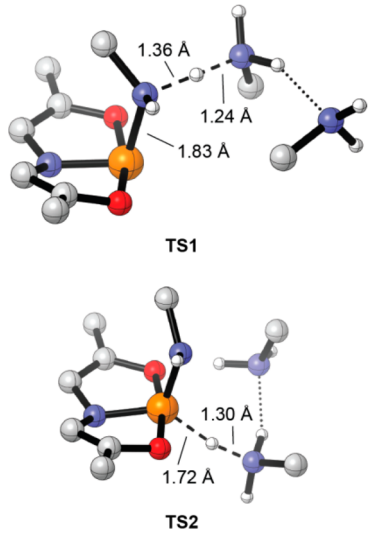

Figure 16. Transition structures along the stepwise electrophilic pathway for N−H oxidative addition to **1** with computed metrics. Hydrogens and *t*-butyl methyl groups were omitted for clarity.

($\Delta H^{\ddagger}$ = 2.4 kcal/mol). **TS2** is the global maximum on the free energy reaction surface, with a $\Delta G^{\ddagger}$ value (18.4 kcal/mol) that is controlled by entropic effects due to organization of the methylamine hydrogen bonding network.

The computed stepwise electrophilic mechanism for N−H oxidative addition is consistent with a number of the key experimental observations, including the high molecularity of the rate law and the corresponding large negative $\Delta S^{\ddagger}$. The apparent negative $\Delta H^{\ddagger}$ is also well-accommodated by the proposed intervention of an initial exothermic P−N adduct.[46] All the intermediates identified by calculations (**INT1**, **INT2**) are endergonic on the free energy surface, which is consistent with the absence of any observable intermediates in the in situ spectroscopy. The endergonic pre-equilibria are energetically subsumed in the apparent activation enthalpy of the subsequent rate controlling proton-transfer via **TS2**. The experimental activation free energy ($\Delta G^{\ddagger}_{expt}{}^{298}$ = 20.7 ± 0.5 kcal/mol) and calculated activation free energy ($\Delta G^{\ddagger}_{calc}{}^{298}$ = 18.4 kcal/mol)

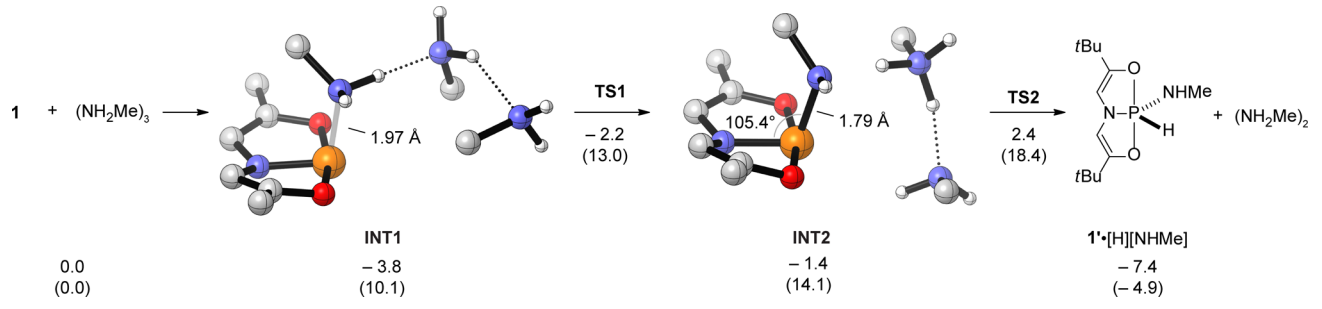

Figure 15. Calculated stepwise electrophilic reaction pathway for the N−H oxidative addition of methylamine to **1** (M06-2X/6-311++G(2d,2p)), with enthalpies (free energies in parentheses) in kcal/mol. Hydrogens and *t*-butyl methyl groups were omitted for clarity on **INT1** and **INT2**.

dx.doi.org/10.1021/ja412469e | J. Am. Chem. Soc. 2014, 136, 4640−4650

are nearly identical and their magnitudes are clearly dominated by entropic contributions. In short, calculation of the electrophilic stepwise mechanism is in good qualitative agreement with experiments.

3. DISCUSSION

The notion that N−H oxidative addition to **1** proceeds via an initial electrophilic step stands in contrast to the anticipated Lewis basicity of trivalent phosphorus compounds but is in line with previous observations from Pudovik[28b] and Quin.[28c] Indeed, the electrophilic or Lewis acid behavior of certain tricoordinate phosphorus compounds is well-established. Diverse phosphorus(III) compounds of the formulas PX_3 and RPX_2 are known to associate Lewis bases including amines,[47] phosphines,[48] and *N*-heterocyclic carbenes.[49] In these structures, the tetracoordinate phosphorus adopts a seesaw shape analogous to the computed structure of the amidophosphoranide intermediate proposed above. Consequently, the starting planar T-shaped geometry of **1** may be considered to predispose the compound to its Lewis acidic function.

In light of the importance of amine-assisted proton transfer to the proposed mechanism for N−H oxidative addition,[50] we speculate that the failure of the reductive elimination experiments described in Section 2.2.2 may have a mechanistic basis. Only in the presence of exogenous amine capable of assisting in proton-shuttling is the amine exchange observed. Absent the exogenous amine, as would be the case in the solid state, reductive elimination would require transit via high energy concerted transition structure like **TS-conc**, and therefore, the N−H addition adducts are thermally robust.

There are parallels between our findings and other N−H oxidative addition systems. A similar two-step complexation/proton-transfer mechanism for E−H oxidative addition has been established in reactions of the tetrelenes (e.g., carbenes,[11] silylenes,[51] and germylenes[52]). This electrophilic activation mode for *p*-block elements bears significant resemblance to the mechanisms that have been advanced for analogous N−H oxidative addition to *d*-block transition metals, where metal ammine complexes are believed to be common intermediates that precede the oxidative addition product along the reaction coordinate.[53] The qualitative functional equivalency between transition metal and main group compounds has been noted.[8−10,54]

4. SUMMARY

The cleavage of the N−H bonds of ammonia, alkylamines, and arylamines by oxidative addition to a geometrically distorted tricoordinate phosphorus compound presented here represents a rare well-characterized example of intermolecular N−H addition to a σ^3-phosphorus compound. These reactions proceed with facility under mild conditions in homogeneous solution to give structurally robust phosphorane adducts. On the basis of mechanistic investigations, we conclude that the observed cleavage of strong N−H bonds by **1** is an entropically controlled, stepwise process initiated by electrophilic activation of the amine substrate to give a phosphoranide intermediate. The rate-determining second step involves a slow amine-assisted proton transfer to furnish the product hydrido amido phosphorane. Investigations delineating the extent to which the planar geometry and corresponding electronic structure of **1** facilitate the electrophilic intermolecular E−H oxidative addition and the potential transferability of this stepwise heterolytic mechanism to other bond making and breaking reactions at tricoordinate phosphorus are ongoing.

5. EXPERIMENTAL SECTION

A full of description of the general experimental methods, including purification and preparation of starting materials, can be found in the Supporting Information.

5.1. Synthesis. *1·[H][NH$_2$].* A nitrogen-flushed 25 mL round-bottom flask equipped with a magnetic stirrer was charged with **1** (200 mg, 0.83 mmol). Ammonia (ca. 5 mL) was condensed into the flask cooled to −78 °C. The suspension was stirred at −78 °C for 30 min, and then warmed to room temperature to remove the excess ammonia, yielding **1**·[H][NH_2] as a yellow solid (214 mg, 0.83 mmol, quantitative yield). ^{1}H NMR (360 MHz, C_6D_6) δ 8.79 (1H, d, J = 812 Hz), 5.35 (2H, d, J = 31 Hz), 1.98 (2H, d, J = 10 Hz), 1.12 (18H, s) ppm. ^{13}C NMR (90 MHz, C_6D_6): δ 149.6 (d, J = 3.6 Hz), 100.4 (d, J = 16.3 Hz), 31.9 (d, J = 3.6 Hz), 27.7 (s) ppm. ^{31}P NMR (145 MHz, C_6D_6): δ −43.5 (dtt, J = 813, 31, 10 Hz) ppm. HRMS (EI) calcd for $[C_{12}H_{23}N_2O_2P]^+$, 258.14972; found, 258.15011. FT-IR (ATR): 3516, 3411, 3128, 2959, 2374, 1655, 1213 cm^{-1}. Anal. Calcd (found) for $C_{12}H_{23}N_2O_2P$: C, 55.83 (55.68); H, 8.98 (8.71); N, 10.85 (10.51); P, 12.00 (12.35).

5.1.2. 1·[H][NH^{n}Pr]. To a solution of *n*-propylamine (17.0 μL, 0.21 mmol) in benzene-d_6 (2 mL) was added **1** (50 mg, 0.21 mmol). The solution was transferred to a sealed J. Young NMR tube and allowed to stand at room temperature for 20 min, yielding **1**·[H][NH^{n}Pr]: (62 mg, 0.21 mmol, quantitative by NMR). Removal of volatiles in vacuo gave **1**·[H][NH^{n}Pr] as a light yellow solid. ^{1}H NMR (360 MHz, C_6D_6) δ 8.89 (1H, d, J = 822.0 Hz), 5.43 (2H, d, J = 30.5 Hz), 2.82 (2H, sextet, J = 8.2 Hz), 2.22 (1H, br), 1.23 (2H, t, 8.6 Hz), 1.16 (18H, s), 0.72 (3H, t, J = 8.8 Hz) ppm. ^{13}C NMR (90 MHz, C_6D_6): δ 149.2 (d, J = 3.6 Hz), 100.5 (d, J = 16.3 Hz), 43.4 (s), 32 (d, J = 3.6 Hz), 27.6 (s), 26.2 (d, J = 3.6 Hz), 11.0 (s) ppm. ^{31}P NMR (145 MHz, C_6D_6): δ −46.4 (dtq, J = 815, 30.5, 12.7 Hz) ppm. HRMS (ESI) calcd for $[C_{15}H_{29}N_2O_2P]^+$, 301.19667; found, 301.19580. FT-IR (ATR): 3436, 2959, 2871, 2372, 1655, 1215 cm^{-1}. Anal. Calcd (found) for $C_{15}H_{29}N_2O_2P$: C, 60.01 (60.03); H, 9.74 (9.31); N, 9.33 (9.19); P, 10.32 (10.05).

5.1.3. 1·[H][NHMes]. To a solution of 2,4,6-trimethylaniline (29.1 μL, 0.21 mmol) in benzene-d_6 (2 mL) was added **1** (50 mg, 0.21 mmol). The solution was transferred to a sealed J. Young NMR tube and heated to 55 °C for 2 h, yielding **1**·[H][NHMes] (78 mg, 0.21 mmol, quantitative yield by NMR). The adduct is stable to column chromatography under nitrogen atmosphere (neutral alumina, 12:1 pentane/DCM). A single crystalline sample was obtained by slow evaporation of a concentrated pentane solution of **1**·[H][NHMes] under an inert atmosphere at −30 °C. ^{1}H NMR (360 MHz, C_6D_6) δ 9.03 (1H, d, J = 839.0 Hz), 6.72 (2H, s), 5.41 (2H, d, 30.7 Hz), 3.43 (1H, d, J = 10.1 Hz), 2.27 (6H, s), 2.13 (3H, s), 0.97 (18H, s) ppm. ^{13}C NMR (90 MHz, C_6D_6): δ 150.0 (d, J = 3.9 Hz), 137.0 (d, J = 3.1 Hz), 135.5 (d, J = 3.6 Hz), 134.6 (d, J = 1.7 Hz), 100.3 (s), 100.1 (s), 31.8 (d, J = 2.6 Hz), 27.3 (s), 20.7 (s), 19.0 (s) ppm. ^{31}P NMR (145 MHz, C_6D_6): δ −48.9 (dtd, J = 839.7, 30.5, 9.6 Hz) ppm. HRMS (ESI) calcd for $[C_{21}H_{33}N_2O_2P]^+$, 376.2358; found, 377.2351. Anal. Calcd (found) for $C_{21}H_{33}N_2O_2P$: C, 67.04 (67.32); H, 8.84 (8.66); N, 7.45 (7.49); P, 8.23 (8.18).

5.2. Calorimetric Methods. Solutions were prepared immediately before each titration by dissolving **1** (1.0 mM) and *n*-propylamine (12.5 mM) in dried, degassed benzene.

ITC experiments were performed using a NanoITC III calorimeter (TA Instruments, New Castle, DE) equipped with hastelloy cells (V = 1.056 mL). Titrations were carried out at 25 °C using a 250 μL syringe at a stirring rate of 250 rpm. The sample cell contained **1** and the reference cell contained benzene. The "heat flow" baseline was allowed to equilibrate once the reference and sample solutions were loaded into the cells. Titrations were run as an incremental series of 6 μL injections of the *n*-propylamine solution into the solution of **1**. Blank experiments were conducted under identical conditions with only solvent in the sample cell to experimentally determine the heat of

dx.doi.org/10.1021/ja412469e | J. Am. Chem. Soc. 2014, 136, 4640−4650

mixing of the *n*-propylamine with the pure solvent. These blanks were subtracted from the experiments with **1** in the cell and integrated to isolate the heat evolved from oxidative addition. Data analysis was performed using NanoAnalyze v2.1 from TA Instruments using the independent binding sites algorithm. The first integrated heat point in the data set is anomalous because the syringe allows for a small amount of *n*-propylamine to mix during equilibration.

5.3. Computational Methods. Geometries were optimized in Gaussian 09[55] using the M06-2X[56] density functional with the 6-311++G(2d,2p) basis set. Optimizations were performed with the continuum CPCM model for acetonitrile.[57] Methylamine was used for a model of *n*-propylamine; the complete compound **1** was modeled. TDDFT calculations were performed with CAMB3LYP[58] since this method provides accurate estimation of charge-transfer excited states. Singlet−triplet gaps, electron affinities, and ionization potentials were calculated using ground-state geometries. See Supporting Information for further details.

■ ASSOCIATED CONTENT

Supporting Information

Additional synthetic procedures including the preparation of **1**; ^{1}H, ^{13}C, and ^{31}P spectra; crystallographic details for **1**·[H][NHMes]; procedures and data for kinetic studies, computational details including Cartesian coordinates for stationary points. This material is available free of charge via the Internet at http://pubs.acs.org.

■ AUTHOR INFORMATION

Corresponding Authors

dhe@chem.byu.edu
radosevich@psu.edu

Notes

The authors declare no competing financial interest.

■ ACKNOWLEDGMENTS

Financial support for this work was provided by the Pennsylvania State University. We thank Profs. Mark Maroncelli and Christine Keating (Penn State) for use of spectrophotometric equipment and Ting-Yi Lai (Penn State) for experimental assistance. D.H.E. thanks BYU and the Fulton Supercomputing Lab.

■ REFERENCES

(1) (a) Lawrence, S. A. *Amines: Synthesis, Properties and Applications*; Cambridge University Press: Cambridge, 2004. (b) van der Vlugt, J. I. *Chem. Soc. Rev.* **2010**, *39*, 2302. (c) Roundhill, D. M. *Chem. Rev.* **1992**, *92*, 1. (d) Casalnuovo, A. L.; Calabrese, J. C.; Milstein, D. *J. Am. Chem. Soc.* **1988**, *110*, 6738. (e) Dorta, R.; Egli, P.; Zucher, F.; Togni, A. *J. Am. Chem. Soc.* **1997**, *119*, 10857.

(2) Zhao, J.; Goldman, A. S.; Hartwig, J. F. *Science* **2005**, *307*, 1080.

(3) (a) Hillhouse, G. L.; Bercaw, J. E. *J. Am. Chem. Soc.* **1984**, *106*, 5472. (b) Hanna, T. E.; Lobkovsky, E.; Chirik, P. J. *Eur. J. Inorg. Chem.* **2007**, 2677.

(4) (a) Ozerov, O. V.; Guo, C.; Fan, L.; Foxman, B. M. *Organometallics* **2004**, *23*, 5573. (b) Roundhill, D. *Inorg. Chem.* **1970**, *9*, 254. (c) Fornies, J.; Green, M.; Spencer, J.; Stone, F. G. A. *J. Chem. Soc., Dalton Trans.* **1977**, 1006. (d) Goel, R. G.; Srivastava, R. C. *J. Organomet. Chem.* **1983**, *244*, 303. (e) Hedden, D.; Roundhill, D. M.; Fultz, W. C.; Rheingold, A. L. *J. Am. Chem. Soc.* **1984**, *106*, 5014. (f) Hartwig, J. F.; Andersen, R. A.; Bergman, R. G. *Organometallics* **1991**, *10*, 1875. (g) Burn, M.; Fickes, M.; Hollander, F.; Bergman, R. *Organometallics* **1995**, *14*, 137. (h) Casalnuovo, A.; Calabrese, J.; Milstein, D. *Inorg. Chem.* **1987**, *26*, 971. (i) Kanzelberger, M.; Zhang, X.; Emge, T. J.; Goldman, A. S.; Zhao, J.; Incarvito, C.; Hartwig, J. F. *J. Am. Chem. Soc.* **2003**, *125*, 13644. (j) Sykes, A. C.; White, P.; Brookhart, M. *Organometallics* **2006**, *25*, 1664. (k) Morgan, E.; MacLean, D. F.; McDonald, R.; Turculet, L. *J. Am. Chem. Soc.* **2009**, *131*, 14234. (l) Huang, Z.; Zhou, J. S.; Hartwig, J. F. *J. Am. Chem. Soc.* **2010**, *132*, 11458.

(5) (a) Sappa, E.; Milone, L. *J. Organomet. Chem.* **1973**, *61*, 383. (b) Armor, J. N. *Inorg. Chem.* **1978**, *17*, 203. (c) Bryan, G.; Johnson, B. F. G.; Lewis, J. *J. Chem. Soc.: Dalton Trans.* **1977**, 1338. (d) Johnson, B. F. G.; Lewis, J.; Odiaka, T. I.; Raithby, P. R. *J. Organomet. Chem.* **1981**, *216*, C56.

(6) Bullock, R. M. *Catalysis without Precious Metals*; Wiley VCH: Weinheim, 2010.

(7) Martin, D.; Soleilhavoup, M.; Bertrand, G. *Chem. Sci.* **2011**, *2*, 389.

(8) Power, P. P. *Nature* **2010**, *463*, 171.

(9) Stephan, D. W.; Erker, G. *Angew. Chem., Int. Ed.* **2010**, *49*, 46.

(10) Frey, G. D.; Lavallo, V.; Donnadieu, B.; Schoeller, W. W.; Bertrand, G. *Science* **2007**, *316*, 439.

(11) (a) Hudnall, T. W.; Moerdyk, J. P.; Bielawski, C. W. *Chem. Commun.* **2010**, *46*, 4288. (b) Moerdyk, J. P.; Blake, G. A.; Chase, D. T.; Bielawski, C. W. *J. Am. Chem. Soc.* **2013**, *135*, 18798. (c) Siemeling, U.; Farber, C.; Bruhn, C.; Leibold, M.; Selent, D.; Baumann, W.; von Hopffgarten, M.; Goedecke, C.; Frenking, G. *Chem. Sci.* **2010**, *1*, 697.

(12) Mizuhata, Y.; Sasamori, T.; Tokitoh, N. *Chem. Rev.* **2009**, *109*, 3479.

(13) (a) Peng, Y.; Ellis, B. D.; Wang, X.; Power, P. P. *J. Am. Chem. Soc.* **2008**, *130*, 12268. (b) Peng, Y.; Guo, J. D.; Ellis, B. D.; Zhu, Z.; Fettinger, J. C.; Nagase, S.; Power, P. P. *J. Am. Chem. Soc.* **2009**, *131*, 16272. (c) Brown, Z. D.; Guo, J. D.; Nagase, S.; Power, P. P. *Organometallics* **2012**, *31*, 3768. (d) For activation of NH_3 at Ga(I), see: Zhu, Z.; Wang, X.; Peng, Y.; Lei, H.; Fettinger, J. C.; Rivard, E.; Power, P. P. *Angew. Chem., Int. Ed.* **2009**, *48*, 2031.

(14) (a) Jana, A.; Schulzke, C.; Roesky, H. W. *J. Am. Chem. Soc.* **2009**, *131*, 4600. (b) Jana, A.; Roesky, H. W.; Schulzke, C.; Samuel, P. P. *Organometallics* **2009**, *28*, 6574.

(15) (a) Jana, A.; Objartel, I.; Roesky, H. W.; Stalke, D. *Inorg. Chem.* **2009**, *48*, 798. (b) Meltzer, A.; Inoue, S.; Präsang, C.; Driess, M. *J. Am. Chem. Soc.* **2010**, *132*, 3038. (c) Wang, W.; Inoue, S.; Yao, S.; Driess, M. *Organometallics* **2011**, *30*, 6490. (d) Myers, T. W.; Berben, L. A. *J. Am. Chem. Soc.* **2013**, *135*, 9988.

(16) (a) Chase, P. A.; Stephan, D. W. *Angew. Chem., Int. Ed.* **2008**, *47*, 7433. (b) Appelt, C.; Slootweg, J. C.; Lammertsma, K.; Uhl, W. *Angew. Chem., Int. Ed.* **2013**, *52*, 4256.

(17) Arduengo, A. J.; Stewart, C. A. *Chem. Rev.* **1994**, *94*, 1215.

(18) Minkin, V. I.; Minyaev, R. M. *Chem. Rev.* **2001**, *101*, 1247.

(19) Arduengo, A. J.; Dixon, D. A. In *Heteroatom Chemistry*; Block, E., Ed.; VCH: New York, 1990; p 47.

(20) Morales-Morales, D.; Jensen, C. M. *The Chemistry of Pincer Compounds*; Elsevier: Amsterdam, 2007.

(21) Herbert, D. E.; Miller, A. D.; Ozerov, O. V. *Chem.—Eur. J.* **2012**, *18*, 7696.

(22) (a) Arduengo, A. J.; Stewart, C. A.; Davidson, F.; Dixon, D. A.; Becker, J. Y.; Culley, S. A.; Mizen, M. B. *J. Am. Chem. Soc.* **1987**, *109*, 627. (b) Arduengo, A. J.; Dixon, D. A.; Stewart, C. A. *Phosphorus Sulfur* **1987**, *30*, 341.

(23) (a) Arduengo, A. J.; Dias, H. V. R.; Calabrese, J. C. *Phosphorus, Sulfur Silicon Relat. Elem.* **1994**, *87*, 1. (b) Arduengo, A. J.; Stewart, C. A.; Davidson, F. *J. Am. Chem. Soc.* **1986**, *108*, 322. (c) Arduengo, A. J.; Lattman, M.; Dixon, D. A.; Calabrese, J. C. *Heteroat. Chem.* **1991**, *2*, 395. (d) Arduengo, A. J.; Lattman, M.; Dias, H. V. R.; Calabrese, J. C.; Kline, M. *J. Am. Chem. Soc.* **1991**, *113*, 1799. (e) Arduengo, A. J.; Dias, H. V. R.; Calabrese, J. C. *J. Am. Chem. Soc.* **1991**, *113*, 7071. (f) Arduengo, A. J.; Dias, H. V. R.; Calabrese, J. C. *Inorg. Chem.* **1991**, *30*, 4880. (g) Arduengo, A. J.; Lattman, M.; Calabrese, J. C.; Fagan, P. J. *Heteroat. Chem.* **1990**, *1*, 407.

(24) Driess, M.; Muresan, N.; Merz, K.; Pach, M. *Angew. Chem., Int. Ed.* **2005**, *44*, 6734.

(25) Dunn, N. L.; Ha, M.; Radosevich, A. T. *J. Am. Chem. Soc.* **2012**, *134*, 11330.

(26) (a) Wolf, R. *Pure Appl. Chem.* **1980**, *52*, 1141. (b) Burgada, R.; Setton, R. In *The Chemistry of Organophosphorus Compounds*; Hartley, F., Ed.; Wiley: Chichester, 1994; Vol. *3*, pp 185−272.
(27) (a) Drozd, G. I.; Ivin, S. S.; Sheluchenko, V. V.; Tetel'baum, B. I.; Luganskii, G. M.; Varshavskii, A. D. *J. Gen. Chem. USSR* **1967**, *37*, 1548. (b) Harman, J. S.; Sharp, D. W. A. *J. Chem. Soc. A* **1970**, 1935. (c) Arnold, D. E. J.; Rankin, D. W. H. *J. Chem. Soc., Dalton Trans.* **1976**, 1130. (d) Rankin, D. W. H.; Wright, J. G. *J. Chem. Soc., Dalton Trans.* **1980**, 2049.
(28) (a) Nifantiev, E. E.; Grachev, M. K.; Burmistrov, S. Y. *Chem. Rev.* **2000**, *100*, 3755 and references therein. (b) Pudovik, M. A.; Mikhailov, Yu. B.; Pudovik, A. N. *Zh. Obshch. Khim.* **1983**, *53*, 1950. (c) Pudovik, M. A.; Terent'eva, S. A.; Il'yasov, A. V.; Chernov, A. N.; Nafikova, A. A.; Pudovik, A. N. *Zh. Obshch. Khim.* **1984**, *54*, 2448. (d) Szewczyk, J.; Quin, L. D. *J. Org. Chem.* **1987**, *52*, 1190.
(29) Houalla, D.; Osman, F .H.; Sanchez, M.; Wolf, R. *Tetrahedron Lett.* **1977**, *35*, 3041.
(30) Bouhadir, G.; Bourissou, D. *Chem. Soc. Rev.* **2004**, *33*, 210.
(31) Kühl, O. *Phosphorus-31 NMR Spectroscopy: A Concise Introduction for the Synthetic Organic and Organometallic Chemist*; Springer-Verlag: Berlin, 2008.
(32) A colorless crystalline sample of **1**·[H][NH_2] may be prepared by sublimation of the crude reaction product in vacuo (ca. 0.8 mmHg) at ambient temperature. An X-ray diffraction study confirms the overall bond connectivities but does not yield a data set of sufficient quality to permit a detailed evaluation of structural metrics.
(33) Ross, M. R.; Martin, J. C. *J. Am. Chem. Soc.* **1981**, *103*, 1234.
(34) Bent, H. A. *Chem. Rev.* **1961**, *61*, 275.
(35) Matsukawa, S.; Kojima, S.; Kajiyama, K.; Yamamoto, Y.; Akiba, K.-Y.; Re, S.; Nagase, S. *J. Am. Chem. Soc.* **2002**, *124*, 13154.
(36) Hoffmann, R.; Howell, J. M.; Muetterties, E. L. *J. Am. Chem. Soc.* **1972**, *94*, 3047.
(37) Weinhold, F.; Landis, C. L. *Valency and Bonding: A Natural Donor-Acceptor Perspective*; Cambridge University Press: Cambridge, 2005.
(38) Luo, Y.-R. *Comprehensive Handbook of Chemical Bond Energies*; CRC Press: Boca Raton, FL, 2007.
(39) Bentrude, W. G.; Kawashima, T.; Keys, B. A.; Garroussian, M.; Heide, W.; Wedegaertner, D. A. *J. Am. Chem. Soc.* **1987**, *109*, 1227.
(40) Fowell, P. A.; Mortimer, C. T. *J. Chem. Soc.* **1959**, 2913.
(41) Fleig, H.; Becke-Goehring, M. *Z. Anorg. Allg. Chem.* **1970**, *376*, 215.
(42) By contrast, concerted (biphilic) oxidative additions to tricoordinate phosphorus have been proposed for the reactions with halogens and peroxides, see: (a) Denney, D. B.; Denney, D. Z.; Chang, B. C.; Marsi, K. L. *J. Am. Chem. Soc.* **1969**, *91*, 5243. (b) Denney, D. B.; Jones, D. H. *J. Am. Chem. Soc.* **1969**, *91*, 5821. (c) Denney, D. B.; Denney, D. Z.; Hall, C. D.; Marsi, K. L. *J. Am. Chem. Soc.* **1972**, *94*, 245. (d) Bartlett, P. D.; Baumstark, A. L.; Landis, M. E.; Lerman, C. L. *J. Am. Chem. Soc.* **1974**, *96*, 5267. (e) Baumstark, A. L.; McCloskey, L. J.; Williams, T. E.; Chrisope, D. R. *J. Org. Chem.* **1980**, *45*, 3593. (f) Clennan, E. L.; Heath, P. C. *J. Org. Chem.* **1981**, *46*, 4105. (g) Lloyd, J. R.; Lowther, N.; Hall, C. D. *J. Chem. Soc., Perkin Trans. 2* **1985**, 245. (h) Wozniak, L.; Kowalski, J.; Chojnowski, J. *Tetrahedron Lett.* **1985**, 4965. (i) Abe, M.; Sumida, Y.; Nojima, M. *J. Org. Chem.* **1997**, *62*, 752.
(43) (a) Shaik, S. S.; Hiberty, P. C. *A Chemist's Guide to Valence Bond Theory*; Wiley-Interscience: Hoboken, NJ, 2008. (b) Su, M.-D. *Inorg. Chem.* **1995**, *34*, 3829.
(44) A nucleophilic mechanism involving initial proton transfer to phosphorus, as in pathway A, is believed to be operative in the oxidative addition of O−H bonds to tricoordinate phosphorus, see: (a) Diallo, O. S.; Brazier, J.-F.; Klaebe, A.; Wolf, R. *Phosphorus Sulfur* **1985**, *22*, 93. (b) Tangour, B.; Malavaud, C.; Boisdon, M. T.; Barrans, J. *Phosphorus Sulfur* **1988**, *40*, 33. (c) Fliss, O.; Bessrour, R.; Tangour, B. *J. Mol. Struct.: THEOCHEM* **2006**, *758*, 225.
(45) Dillon, K. B. *Chem. Rev.* **1994**, *94*, 1441.
(46) Negative activation enthalpies arising from stepwise processes have been described in other systems: (a) Kisalev, V.; Miller, J. *J. Am. Chem. Soc.* **1975**, *97*, 4036. (b) Turro, N. J.; Lehr, G. F.; Butcher, J. A; Moss, R. A.; Guo, W. *J. Am. Chem. Soc.* **1982**, *104*, 1754. (c) Turro, N. J.; Hrovat, D. A.; Gould, I. R.; Padwa, A.; Dent, W.; Rosenthal, R. J. *Angew. Chem., Int. Ed. Engl.* **1983**, *22*, 625. (d) Houk, K. N.; Rondan, N. G. *J. Am. Chem. Soc.* **1984**, *106*, 4293. (e) Kapinus, E. I.; Rau, H. *J. Phys. Chem. A.* **1998**, *102*, 5569.
(47) (a) Holmes, R. R. *J. Phys. Chem.* **1960**, *64*, 1295. (b) Holmes, R. R.; Wagner, R. P. *Inorg. Chem.* **1968**, *2*, 384. (c) Cong, C. B.; Gence, G.; Garrigues, B.; Koenig, M.; Munoz, A. *Tetrahedron* **1979**, *35*, 1825. (d) Carré, F.; Chuit, C.; Corriu, R. J. P.; Monforte, P.; Nayyar, N. K.; Reyé, C. *J. Organomet. Chem.* **1995**, *499*, 147. (e) Chuit, C.; Reyé, C. *Eur. J. Inorg. Chem.* **1998**, 1847.
(48) (a) Holmes, R. R.; Bertaut, E. F. *J. Am. Chem. Soc.* **1958**, *80*, 2980. (b) Müller, G.; Matheus, H.-J.; Winkler, M. *Z. Naturforsch.* **2001**, *56b*, 1155. (c) Wawrzyniak, P.; Fuller, A. L.; Slawin, A. M. Z.; Kilian, P. *Inorg. Chem.* **2009**, *48*, 2500. (d) Surgenor, B. A.; Bühl, M.; Slawin, A. M. Z.; Woolins, J. D.; Kilian, P. *Angew. Chem., Int. Ed.* **2012**, *51*, 10150.
(49) (a) Wang, Y.; Xie, Y.; Wei, P.; King, R. B.; Schaefer, I.; Schleyer, P. v. R.; Robinson, G. H. *J. Am. Chem. Soc.* **2008**, *130*, 14970. (b) Back, O.; Donnadieu, B.; Parameswaran, P.; Frenking, G.; Bertrand, G. *Nat. Chem.* **2010**, *2*, 369. (c) Wang, Y.; Xie, Y.; Abraham, M. Y.; Gilliard, R. J.; Wei, P.; Schaefer, H. F.; Schleyer, P. v. R.; Robinson, G. H. *Organometallics* **2010**, *29*, 4778. (d) Wang, Y.; Xie, Y.; Abraham, M. Y.; Wei, P.; Schaefer, H. F.; Schleyer, P. v. R.; Robinson, G. H. *Chem. Commun.* **2011**, *47*, 9224. (e) Wang, Y.; Robinson, G. H. *Dalton Trans.* **2012**, *41*, 337.
(50) For examples of amine base-catalysis on O−H oxidative addition to tricoordinate phosphorus, see: (a) Ref 44a. (b) Van Lier, J. J. C.; Hermans, R. J. M.; Buck, H. M. *Phosphorus Sulfur* **1984**, *19*, 173.
(51) (a) Steele, K. P.; Weber, W. P. *Inorg. Chem.* **1981**, *20*, 1302. (b) Raghavachari, K.; Chandrasekhar, J.; Gordon, M. S.; Dykema, K. J. *J. Am. Chem. Soc.* **1984**, *106*, 5853. (c) Oka, K.; Nakao, R. *Res. Chem. Intermed.* **1990**, *390*, 7. (d) Baggott, J. E.; Blitz, M. A.; Frey, H. M.; Lightfoot, P. D.; Walsh, R. *Int. J. Chem. Kinet.* **1992**, *24*, 127. (e) Su, S.; Gordon, M. S. *Chem. Phys. Lett.* **1993**, *204*, 306. (f) Lee, S. Y.; Boo, B. H. *J. Mol. Struct.* **1996**, *366*, 79. (g) Heaven, M. W.; Metha, G. F.; Buntine, M. A. *Aust. J. Chem.* **2001**, *54*, 185. (h) Becerra, R.; Cannady, J. P.; Walsh, R. *J. Phys. Chem. A* **2003**, *107*, 11049. (i) Tokitoh, N.; Ando, W. Silylenes (and Germylenes, Stannylenes, Plumbylenes). In *Reactive Intermediate Chemistry*; Moss, R. A., Platz, M. S., Jones, M., Eds.; Wiley: Hoboken, NJ, 2004; pp 669−670. (j) Moiseev, A. G.; Leigh, W. J. *Organometallics* **2007**, *26*, 6277. (k) Leigh, W. J.; Kostina, S. S.; Bhattacharya, A.; Moiseev, A. G. *Organometallics* **2010**, *29*, 662. (l) Kostina, S. S.; Singh, T.; Leigh, W. J. *J. Phys. Org. Chem.* **2011**, *24*, 937. (m) Becerra, R.; Cannady, J. P.; Walsh, R. *J. Phys. Chem. A* **2011**, *115*, 4231.
(52) (a) Peng, Y.; Guo, J. D.; Ellis, B. D.; Zhu, Z.; Fettinger, J. C.; Nagase, S.; Power, P. P. *J. Am. Chem. Soc.* **2009**, *131*, 16272. (b) Brown, Z. D.; Guo, J.-D.; Nagase, S.; Power, P. P. *Organometallics* **2012**, *31*, 3768.
(53) (a) Park, S.; Johnson, M. P.; Roundhill, D. M. *Organometallics* **1989**, *8*, 1700. (b) Blomberg, M. R. A.; Siegbahn, P. E. M.; Svensson, M. *Inorg. Chem.* **1993**, *32*, 4218. (c) Schulz, M.; Milstein, D. *Chem Commun.* **1993**, 318. (d) Macgregor, S. A. *Organometallics* **2001**, *20*, 1860.
(54) (a) Hoffmann, R. *Angew. Chem., Int. Ed.* **1982**, *10*, 711. (b) Halpern, J. *Chem. Eng. News* **1966**, *44*, 68.
(55) Frisch, M. J.; Trucks, G. W.; Schlegel, H. B.; Scuseria, G. E.; Robb, M. A.; Cheeseman, J. R.; Scalmani, G.; Barone, V.; Mennucci, B.; Petersson, G. A.; Nakatsuji, H.; Caricato, M.; Li, X.; Hratchian, H. P.; Izmaylov, A. F.; Bloino, J.; Zheng, G.; Sonnenberg, J. L.; Hada, M.; Ehara, M.; Toyota, K.; Fukuda, R.; Hasegawa, J.; Ishida, M.; Nakajima, T.; Honda, Y.; Kitao, O.; Nakai, H.; Vreven, T.; Montgomery, J. A., Jr.; Peralta, J. E.; Ogliaro, F.; Bearpark, M.; Heyd, J. J.; Brothers, E.; Kudin, K. N.; Staroverov, V. N.; Kobayashi, R.; Normand, J.; Raghavachari, K.; Rendell, A.; Burant, J. C.; Iyengar, S. S.; Tomasi, J.; Cossi, M.; Rega, N.; Millam, J. M.; Klene, M.; Knox, J. E.; Cross, J. B.; Bakken, V.; Adamo, C.; Jaramillo, J.; Gomperts, R.; Stratmann, R. E.; Yazyev, O.; Austin, A. J.; Cammi, R.; Pomelli, C.; Ochterski, J. W.; Martin, R. L.;

Morokuma, K.; Zakrzewski, V. G.; Voth, G. A.; Salvador, P.; Dannenberg, J. J.; Dapprich, S.; Daniels, A. D.; Farkas, O.; Foresman, J. B.; Ortiz, J. V.; Cioslowski, J.; Fox, D. J. *Gaussian 09*, revision B.01; Gaussian, Inc.: Wallingford, CT, 2009.
(56) (a) Zhao, Y.; Truhlar, D. G. *Theor. Chem. Acc.* **2008**, *120*, 215. (b) Zhao, Y.; Truhlar, D. G. *Acc. Chem. Res.* **2008**, *41*, 157.
(57) Scalmani, G.; Frisch, M. J. *J. Chem. Phys.* **2010**, *132*, 114110.
(58) Yanai, T.; Tew, D.; Handy, N. *Chem. Phys. Lett.* **2004**, *393*, 51.